



# Modulating flavanone compound for reducing the bitterness and improving dietary fiber, physicochemical properties, and anti-adipogenesis of green yuzu powder by enzymatic hydrolysis

Hyeon-Jun Seong<sup>a</sup>, Hyeong Kim<sup>b</sup>, Jeong-Yong Cho<sup>a</sup>, Kwang-Yeol Yang<sup>c</sup>, Seung-Hee Nam<sup>a,d,\*</sup>

<sup>a</sup> Department of Integrative Food, Bioscience and Biotechnology, Chonnam National University, Gwangju 61186, Republic of Korea

<sup>b</sup> Institute of Food Industrialization, Institutes of Green Bioscience & Technology, Center for Food and Bioconvergence, Seoul National University, Pyeongchang-gun, Gangwon-do 25354, Republic of Korea

<sup>c</sup> Department of Applied Biology, College of Agriculture and Life Science, Chonnam National University, Gwangju 61186, Republic of Korea

<sup>d</sup> Institute of Agricultural and Life Science Technology, Chonnam National University, Gwangju, Republic of Korea

## ARTICLE INFO

### Keywords:

*Aspergillus oryzae* NYO-2  
Cellulase  
Dietary fiber  
Green yuzu  
Naringinase

## ABSTRACT

Yuzu (*Citrus junos* Sieb.) is a peel-edible fruit with a pleasant aroma, but its bitter taste can impact consumer appeal. In this study, an efficient enzymatic method reduced bitterness in green yuzu powder (GYP). Cellulase KN and naringinase from *Aspergillus oryzae* NYO-2 significantly decreased naringin and neohesperidin content by over 87 %, while increasing total dietary fiber and soluble dietary fiber by up to 10 % and 51 %, respectively. Insoluble dietary fiber decreased by up to 22 %. Cellulose, hemicellulose, lignin, and pectin contents in enzyme-treated YP decreased by 1.15–2.00-fold, respectively. Enzyme-treated GYP exhibited improved physicochemical properties, including enhanced solubility, oil-holding capacity, and water swelling capacities. 3T3-L1 cells treated with cellulase-treated GYP and naringinase-treated GYP showed lower lipid accumulation and higher lipolysis capability than GYP, along with decreased fatty acid synthase contents. These findings suggest that enzyme-treated GYP holds potential as a functional ingredient in the food industry.

## 1. Introduction

Yuzu (*Citrus junos* Sieb.) is a peel-edible fruit found in Japan, China, and Korea. It is distinguished from other citrus fruits by having a potent, distinctive aroma and is well-recognized for the delightful fragrance of its outer peel. Yuzu contains high levels of bioactive compounds, such as flavonoids, phenolic compounds, organic acids, and minerals that contribute to its biological activities, including antioxidant, antidiabetic, anti-inflammatory, neuroprotective, anticarcinogenic, and anti-hypertensive activities (Kim et al., 2013; Lee, Kim, Pyeon, Jeong, Cho, & Nam, 2022; Nam, et al., 2021). Moreover, yuzu peel is rich in dietary fiber, primarily composed of cellulose, polysaccharides, lignin, and proteins that give their superior physicochemical properties, enhance their biodegradable properties, and contribute to human health benefits as dietetic ingredients (Lv, Liu, Zhang, & Wang, 2017; Karra, et al.,

2020; Nam, et al., 2021). Therefore, yuzu has been used to produce various food products, such as fruits, sugar-pickled yuzu tea, aroma and flavor additives, and natural ingredients in biodegradable polymers and packaging materials (Nam, et al., 2021). Green yuzu, the immature fruit of yuzu, has gained attention recently due to its higher flavonoid content than mature yuzu. Specifically, naringin and neohesperidin are 2.5–4.0 times more abundant than in mature yuzu (Nam, et al., 2021). However, green yuzu is known for its bitter taste, which limits its acceptability in foods.

Various chemical, mechanical, enzymatic, and fermentation methods have been used alone or in combinations to diminish the bitter taste of flavonoid-rich citrus fruit-derived extracts. Among them, enzymatic methods have been gaining the attention of researchers due to their simplicity, high yields of target products, and high recovery yields of products. Enzymatic methods have been widely used to modify the

**Abbreviations:** ADF, acid detergent fiber; CGYP, commercial enzyme (Cellulase KN)-treated green yuzu powder; E-tongue, electronic tongue; FAS, fatty acid synthase; FT-IR, Fourier transform infrared; GYP, green yuzu powder; IDF, insoluble dietary fiber; MGYP, microbial enzyme (naringinase from *Aspergillus oryzae* NYO-2)-treated green yuzu powder; NDF, neutral detergent fiber; OHC, oil holding capacity; PCA, principal component analysis; PDI, polydispersity index; SDF, soluble dietary fiber; FE-SEM, Field emission scanning electron microscopy; TDF, total dietary fiber; WHC, water holding capacity; WSC, water swelling capacity.

\* Corresponding author at: Institute of Agricultural Life Science Technology, Chonnam National University, Gwangju 61186, Republic of Korea.

E-mail address: [namsh1000@jnu.ac.kr](mailto:namsh1000@jnu.ac.kr) (S.-H. Nam).

<https://doi.org/10.1016/j.fochx.2024.101329>

Received 7 December 2023; Received in revised form 21 March 2024; Accepted 21 March 2024

Available online 27 March 2024

2590-1575/© 2024 The Authors. Published by Elsevier Ltd. This is an open access article under the CC BY-NC license (<http://creativecommons.org/licenses/by-nc/4.0/>).

physical and functional properties of various food and agricultural products (Yu, Bei, Zhao, Li, & Cheng, 2018; Zhang, Bai, & Zhang, 2011; Zhang, Qi, Zeng, Huang, & Yang, 2020; Zheng & Li, 2018). Yu et al. (2018) found that modification of the insoluble dietary fiber (IDF) in carrot pomace by combined cellulase and xylanase treatment increased the soluble dietary fiber (SDF) content to 15.07 %, which was 8 times higher than untreated carrot pomace. In another study, Ma et al. (2016) showed that combined laccase and cellulase treatment increased the contents of SDF, free sugars, and uronic acid in carrot pomace and decreased its particle size (Ma, Ren, Diao, Chen, Qiao, & Liu, 2016). To reduce the bitterness of flavonoid-rich citrus-derived extracts, previous studies have focused mainly on using naringinase to hydrolyze purified naringin and neohesperidin (Lee, Huh, Nam, Moon, & Lee, 2012; Seong, et al., 2023). However, little is known about the effects of enzymes on citrus fruits' physicochemical, structure, and biochemical properties.

Therefore, this study aims to evaluate the effectiveness of enzyme treatments in reducing the bitterness of green yuzu powder (GYP) and to investigate its physical and functional properties. Nine commercial enzymes and two *Aspergillus oryzae*-derived naringinase enzymes were screened for their ability to hydrolyze naringin and neohesperidin in GYP. The effects of enzyme concentration, GYP concentration, and reaction time on the hydrolysis of naringin and neohesperidin were determined by varying one factor at a time. Field emission scanning electron microscopy (FE-SEM) and Fourier transform infrared (FT-IR) spectroscopy analysis were performed to investigate the changes in GYP morphology induced by enzyme treatment. The influence of enzyme treatment on the biochemical composition, such as the dietary fiber content and composition, and the physicochemical properties, including the particle size distribution, solubility, water holding capacity (WHC), water swelling capacity (WSC), and oil holding capacity (OHC) of GYP were measured. Furthermore, the effects of enzyme-treated GYP on lipid accumulation, glycerol release, and fatty acid synthase (FAS) contents in mouse 3T3-L1 cells were analyzed. This study's results would provide an effective method for enhancing the functional properties of green yuzu for food industrial applications.

## 2. Materials and methods

### 2.1. Materials

Green yuzu fruits were harvested in August 2022 at the Fruit Research Center of Jeonnam Agricultural Research & Extension Services (Heanam, Jeonnam Province, Korea, 34° 34' 16"N, 126° 35' 56' E). Naringin, neohesperidin, narirutin, hesperidin, prunin, hesperetin-7-O-glucoside, epigallocatechin-3-gallate (EGCG), naringenin, sodium dodecyl sulfate (SDS), ethylenediaminetetraacetic acid (EDTA), and hesperetin were bought from Sigma-Aldrich Co., LLC (St. Louis, MO, USA). The 3-(4,5-dimethyl-2-thiazolyl)-2,5-diphenyl-2H-tetrazolium bromide (MTT) was purchased from Thermo Fisher Scientific (Waltham, MA, USA). Mouse 3T3-L1 cells were obtained from the American Type Culture Collection (ATCC, Rockville, MD, USA). Dulbecco's modified Eagle's medium (DMEM), fetal bovine serum (FBS), and newborn calf serum (BCS) were purchased from Gene Depot (Barker, TX, USA). Pectines XXL, Rapidase Press, Rapidase Fiber, Plantase CP, Plantase UF, Plantase PR, Pectinex Ultra SP-L, Cellulase KN, and Pectinex 100L (Table S1) were bought from Vision Corp. (Seoul, Korea). Naringinase from *Aspergillus oryzae* NYO-2 (KCTC 14898BP) and naringinase from *A. oryzae* 6377 (KCTC 6377) (Table S2) were obtained and prepared as described in our previous report (Seong et al., 2023). All other substances used in the experiment were of analytical grade or higher.

### 2.2. Preparation of green yuzu powder

Whole green yuzu fruits were half-sliced and lyophilized (FD8512 freeze dryer, IlshinBioBase, Korea). Lyophilized green yuzu was ground in a grinder. The ground powder was passed through a 60-mesh sieve to

obtain particles of similar size and designated as GYP, which was used for the experiment.

### 2.3. Enzyme screening

Eleven enzymes, including 9 commercial enzymes and 2 naringinase enzymes were screened for their ability to hydrolyze naringin and neohesperidin in GYP by adding 0.1 % (v/v) enzyme into the reaction mixture composed of 50 mg of lyophilized GYP in 20 mM sodium acetate buffer (pH 5.4). The reaction was incubated at 37 °C for 12 h and heating at 100 °C for 15 min. Then, the reaction mixture was filtered with a 0.2 µm Minisart syringe filter (Sartorius, Gottingen, Germany) and used for high-performance liquid chromatography (HPLC) analysis as reported previously (Seong et al., 2023). A 20-µL sample was injected into the C<sub>18</sub> column (4.6 × 250 mm, 5 µm; ZORBAX Eclipse Plus, Agilent Technologies, Inc., Santa Clara, CA, USA) connected to an Agilent 1216 Infinity LC system. The column temperature was set to 35 °C. Chromatographic separations were achieved using a binary mobile phase composed of 0.1 % (v/v) formic acid (A) and acetonitrile (B) with the following elution gradient: 20 % B from 0 to 4.9 min, 40 % B from 5 to 10 min, 50 % B from 10.1 to 15 min, 70 % B from 15.1 to 20 min, and 100 % B from 20.1 to 25 min. Naringin and neohesperidin were detected under UV<sub>280nm</sub>. Flavanone compounds at 0.5–5.0 mg/mL were used as standards (Table S3). Based on the above screening, one commercial enzyme and one *A. oryzae*-derived naringinase were selected among these tested enzymes for further study.

### 2.4. Selection of hydrolysis conditions

The hydrolyzed conditions, including enzyme concentration, GYP concentration, and the reaction time on the contents of naringin and neohesperidin in GYP by using Cellulase KN and naringinase from isolated *A. oryzae* NYO-2 were studied by varying one factor at a time. The effect of enzyme concentration was evaluated by adding different concentrations of enzyme (0–0.25 %, v/v) to the reaction mixture composed of 50 mg of lyophilized GYP in 20 mM sodium acetate buffer (pH 5.4) and incubated at 37 °C for 12 h. The effect of GYP at 1.0–10.0 % (w/v) mixed with 0.1 % commercial enzyme or 0.25 % naringinase NYO-2 and reacted time for 12 h was examined. The effect of reaction times was studied by incubating the reaction mixture of 0.1 % commercial enzyme or 0.25 % naringinase NYO-2 and 5 % GYP at different times (0–24 h). Then, naringin and neohesperidin content in the reaction mixture were analyzed by HPLC, as described above (section 2.3).

### 2.5. Analyses of dietary fiber

#### 2.5.1. Total dietary fiber, soluble dietary fiber, and insoluble dietary fiber analyses

Dietary fiber was analyzed according to the method described by Prosky (Prosky et al., 1988). To determine insoluble dietary fiber (IDF) content, 1 g of sample in MES-Tris buffer was treated with thermostable α-amylase at 95 °C, protease at 60 °C, and amyloglucosidase at 60 °C. The resulting residue was washed with 75 % ethanol, 95 % ethanol, and acetone. After drying for 12 h, it was measured for fiber content, excluding protein and ash. Soluble dietary fiber (SDF) was determined by adding 4 volumes of 95 % ethanol to the filtrate to precipitate soluble materials for 1 h. The mixture was filtered through tared fritted glass crucibles. The dry weight (DW) of the precipitate was measured. Total dietary fiber (TDF) content was calculated as the sum of IDF and SDF. Ash content was analyzed by the official methods of analysis (AOAC) method, and crude protein content was quantified using the Kjeldahl method with a conversion factor of 6.25 (Lynch & Barbano, 1999).

#### 2.5.2. Analyses of acid detergent fiber and neutral detergent fiber

To analyze the acid detergent fiber (ADF) content, a 0.5 g sample was mixed with 200 mL of acid detergent containing 20 g acetyl trimethyl

ammonium bromide in 1 L of 1 N H<sub>2</sub>SO<sub>4</sub>, followed by stirring at 100 °C for 1 h. The resulting residue was washed with 40 mL of distilled water (90 °C) and 40 mL of acetone until the color disappeared and then dried at 105 °C for 12 h and weighed. ADF was calculated by dividing the residue's weight by the sample's weight. To determine the neutral detergent fiber (NDF) content, a 0.5 g sample was mixed with 200 mL of a neutral detergent comprised of 6 g SDS, 3.72 g EDTA, 1.36 g sodium borate, 0.91 g disodium hydrogen phosphate, and 2 mL of 2-ethoxy ethanol, followed by stirring at 100 °C for 1 h. After that, the residue was thoroughly cleaned with 40 mL of distilled water at 90 °C and 40 mL of acetone until no longer colored. The residue was dried at 105 °C for 12 h before being weighed. NDF was calculated by dividing the residue's weight by the sample's weight.

### 2.5.3. Analyses of lignin, cellulose, hemicellulose, and pectin contents

The cellulose, hemicellulose, lignin, and pectin contents of GYP, commercial enzyme (Cellulase KN)-treated green yuzu powder (CGYP), and naringinase NYO-2-treated green yuzu powder (MGYP) were analyzed using a modified protocol from our previous study (Nam et al., 2021). To determine the lignin content, 15 mL of 72 % H<sub>2</sub>SO<sub>4</sub> was added to 0.5 g of sample, stirred for 2 h. The suspension was diluted with distilled water until the H<sub>2</sub>SO<sub>4</sub> concentration reached 3 % and kept at 98 °C for 3 h to precipitate. The precipitate was washed with hot water and dried at 105 °C. The lignin content was determined by dividing the precipitate weight by the weight of the initial sample. Cellulose content was calculated as the difference between the ADF and lignin contents, and hemicellulose was determined as the difference between the NDF and ADF content. Pectin content was analyzed using a pectin identification kit (Megazyme, Ireland) according to the manufacturer's guidelines. Cellulose at 0.01–10 mg/mL, hemicellulose at 0.01–10 mg/mL, lignin at 0.01–5.0 mg/mL, and pectin at 0.01–1.0 mg/mL were used as standards (Table S3).

### 2.5.4. Analyses of glucose, fructose, rhamnose, sucrose, xylose, and galacturonic acid

The glucose, fructose, rhamnose, sucrose, xylose, and galacturonic acid in GYP, CGYP, and MGYP were analyzed by an HPLC method. The sample was filtered through a 0.2- $\mu$ m Minisart syringe filter and then injected to the carbohydrate column (4.6  $\times$  250 mm, 5  $\mu$ m, ZORBAX Eclipse, Agilent Technologies, Inc.) connected to a 1216 Infinity LC with a refractive index detection (RID)-10A detector. The column temperature was set at 40 °C. Water containing 0.1 % phosphoric acid was used as the mobile phase at a flow rate of 0.6 mL/min for 45 min. Standard curves for glucose, fructose, sucrose, rhamnose, and galacturonic acid were constructed, which showed linearity values ( $R^2$ ) over 0.97.

## 2.6. Physicochemical properties

### 2.6.1. Particle size, polydispersity index, and zeta potential

To ensure uniform particle size, GYP, CGYP, and MGYP were passed through a 60-mesh sieve. The particles, polydispersity index (PDI), and surface charge (zeta potential) of the resuspensions containing 0.1 % (w/v) GYP, CGYP, and MGYP in deionized water were analyzed at 25 °C using an electrophoretic light scattering spectrophotometer (ELS-Z2, Otsuka Electronics Co., Osaka, Japan).

### 2.6.2. Water holding capacity analysis

Water holding capacity (WHC) was performed according to the method described by Cheng, Zhang, Hong, Li, Li, & Gu, 2017, with slight modifications. The dried sample (0.5 g) was mixed with 10 mL of water and kept at 25 °C for 24 h. Then, the mixture was centrifuged at 4000  $\times$  g for 15 min (Combi 514R centrifuge, Hanil Scientific Inc., Gimpo, Korea). The supernatant was discarded, and the pellet was weighed. The WHC was calculated using the following equation.

$$WHC(g/g) = (W_0 - W_1)/W_1 \quad (1)$$

where  $W_0$  represents the weight of the dried sample, and  $W_1$  represents the weight of the pellet.

### 2.6.3. Oil holding capacity analysis

Oil holding capacity (OHC) was determined by centrifugation (4000g, 15 min) of a suspension of 0.5 g of the dried sample with 5 mL of olive oil that has been mixed at 4 °C for 1 h. The supernatant was discarded, and the pellet was weighed. The OHC was calculated using the following equation.

$$OHC(g/g) = (W_0 - W_1)/W_1 \quad (2)$$

where  $W_0$  represents the weight of the pellet, and  $W_1$  represents the weight of the dried sample.

### 2.6.4. Solubility analysis

Solubility was analyzed according to our previous report (Jeong, et al., 2023). The sample (0.5 g) was mixed with 10 mL of water and then shaken at 60 rpm for 60 min. The pellet obtained after centrifugation at 4000  $\times$  g for 15 min was dried at 105 °C. The pellet was weighed, and the solubility was calculated using the following equation.

$$Solubility(\%) = (1 - W_1/W_0) \times 100 \quad (3)$$

where  $W_1$  represents the weight of the sample after drying, and  $W_0$  represents the initial weight of the sample.

### 2.6.5. Water swelling capacity analysis

Water swelling capacity (WSC) was performed according to the method described by Zhang, Bai, & Zhang, 2011 with slight modifications. The dried sample (0.5 g) was mixed with 10 mL of water at 4 °C for 18 h. The volume occupied by the sample was measured, and the WSC was calculated using the following equation,

$$WSC(mL/g) = (V_1 - V_2)/W_2 \quad (4)$$

$V_1$  represents the volume of the hydrated sample,  $V_2$  represents the volume of the dried sample, and  $W_1$  represents the weight of the dried sample.

### 2.6.6. Hunter's color value

Hunter's color value was analyzed with a color spectrophotometer (handheld color spectrophotometer 45/0 NS 800, Shenzhen 3nh Technology Co., Ltd, Shenzhen, China) to determine  $L^*$  (lightness),  $a^*$  (redness),  $b^*$  (yellowness), and  $\Delta E^*$  (total color difference). The instrument was calibrated against a standard white plate ( $L^* = 96.39$ ,  $a^* = 0.43$ ,  $b^* = 1.33$ ). The value of  $\Delta E^*$  was calculated using the following equation:

$$\Delta E = \sqrt{(L - L_0)^2 - (a - a_0)^2 - (b - b_0)^2} \quad (5)$$

## 2.7. Structural characterization

### 2.7.1. Field emission scanning electron microscopy analysis

The surface of GYP, CGYP, and MGYP were observed using a field emission scanning electron microscopy (FE-SEM) (Gemini 500, Zeiss, Oberkochen, Germany). The dried samples were coated with platinum and observed at an accelerating voltage of 15 kV and a magnification of 1,000 and 2,000 times, respectively.

### 2.7.2. Fourier transform infrared spectra analysis

The effects of enzyme treatment on the functional groups of GYP were analyzed using an Fourier transform infrared spectra (FT-IR) spectrophotometer (Frontier-89063, PerkinElmer, Inc., Waltham, MA, USA) equipped with a MIR TGS detector. The spectra were read in absorbance mode from 4000 to 500  $\text{cm}^{-1}$ .

## 2.8. Analysis of bitterness

The bitterness of GYP, CGYP, and MGYP were analyzed using an electronic tongue (E-tongue, AstreeII, Alpha MOS, Toulouse, France) with sensors, including salty, sweet, umami, bitter, sour, and auxiliary tastes in the range of 0 to 10. The sample (5 g) was dissolved in 100 mL water and measured five times for 120 s each time using a sensory analyzer. The taste profile of each sample was analyzed using discriminant function analysis (DFA) with the AlphaSoft version 17 software (Alpha MOS, Toulouse, France).

## 2.9. Analyses of anti-lipid accumulation, glycerol, and fatty acid synthase content on 3T3-L1 cells

### 2.9.1. Cell cytotoxicity

Mouse 3T3-L1 cells were maintained in DMEM supplemented with 10 % BCS and 1 % penicillin–streptomycin and were incubated at 37 °C under a 5 % CO<sub>2</sub> atmosphere until 70 % confluence. Mouse 3T3-L1 cells were seeded at  $2 \times 10^4$  cells/well in a 24-well plate for 96 h and used to determine preadipocyte and adipocyte viability when treated with GYP, CGYP, and MGYP. For the preadipocyte viability assay, the cells were treated with different concentrations of the samples (0–250 µg/mL) for 24 h. For adipocyte viability assay, cells in the 24-well plate were replaced with DMEM containing 10 % FBS, 0.5 mM IBMX, 1 µM dexamethasone, and 1 µg/mL insulin and cultured for 72 h to induce differentiation. The medium was then replaced with an insulin medium consisting of DMEM, 10 % FBS, and 1 µg/mL insulin. After 72 h, the cell medium was replaced with DMEM containing 10 % FBS, and the cells were cultured for 72 h to complete differentiation into mature adipocytes. Cell viability was determined using the Ez-Cytox kit (EZ-3000, DoGenBio, Seoul, Korea) by adding 100 µL of a solution containing 90 µL DMEM and 10 µL Ez-Cytox to each well and incubated at 37 °C for 2.5 h. The plate was read at 450 nm using a spectrophotometer (BioTek Instruments, Winooski, VT, USA). Cell viability was expressed as cell survival rate compared to the control.

### 2.9.2. Lipid accumulation by oil red O staining

GYP, CGYP, and MGYP were added to the medium at concentrations of 10, 20, and 40 µg/mL at each stage of the adipogenesis process. EGCG at 50- and 100 µM was used as the positive control. Lipid droplets in mature adipocytes were stained using the Oil Red O staining method. The cells were fixed in 10 % formalin for 1 h, washed with PBS, and dried. They were stained with Oil Red O solution in isopropanol for 1 h, washed with water, and imaged using an inverted contrast phase microscope (Nikon, Tokyo, Japan). After adding isopropanol to the stained plate, lipid content was measured at 510 nm using a spectrophotometer (BioTek Instruments).

### 2.9.3. Analysis of free glycerol content

To investigate the effect of GYP, CGYP, and MGYP on lipolysis, mature 3T3-L1 adipocytes were treated with these compounds at concentrations of 10, 20, and 40 µg/mL for 72 h. The free glycerol released in the medium was measured using the EZ-free glycerol assay kit (DGF-GC100, DoGenBio, Seoul, Korea). Results were expressed as the amount of released free glycerol compared with the control group.

### 2.9.4. Fatty acid synthase content

For fatty acid synthase (FAS) analysis, GYP, CGYP, and MGYP at 20 µg/mL were used to treat mouse 3T3-L1 cells at every stage of the adipogenesis process. Then, 200 µL of radioimmunoprecipitation assay (RIPA) buffer was added to each well. The mixture was collected and centrifuged at  $9000 \times g$  for 10 min at 4 °C to obtain the supernatant. The supernatant was used to determine the FAS content using the fatty acid ELISA kit (CUSABIO, Houston, TX, USA) according to the manufacturer's guidelines. The concentration of fatty acid synthase was calculated based on the standard curve obtained from the kit.

## 2.10. Statistical analysis

Experimental results were expressed as triplicate experiments' mean  $\pm$  standard deviation (SD). Data were analyzed with SPSS version v26.0 (IBM Corp., Chicago, IL, USA), using analysis of variance (ANOVA) followed by Duncan's post hoc test. Differences in lipid accumulation and free glycerol release in 3T3-L1 cells among groups were tested by ANOVA followed by Turkey's multiple comparisons test. A significant difference was considered as  $p < 0.05$  by ANOVA. MetaboAnalyst 5.0, an online tool (<https://www.metaboanalyst.ca>), performed the principal component analysis (PCA) and correlation analysis.

## 3. Results and discussion

### 3.1. Screening of enzymes hydrolyzing naringin and neohesperidin in green yuzu powder

Although flavonoid compounds in yuzu such as narirutin, naringin, hesperidin, and neohesperidin, which are found in the highest amount in green yuzu, exhibit numerous biological activities, including antioxidant, anti-inflammatory, antiviral, and neuroprotection effects (Benavente-Garcia & Castillo, 2008; Nam, et al., 2021; Seong et al., 2023), they are known as bitter compounds that can affect the sensory quality of products (Kore & Chakraborty, 2015; Lee, Kim, Pyeon, Jeong, Cho, & Nam, 2022). Our previous study reported that the combination of three enzymes, including cellulase KN from *Aspergillus niger*, plantase UF from *Aspergillus niger*, and cellulase from isolated *Leuconostoc mesenteroides* NY203 decreased these flavonoid compounds in GYP by reducing 50 % of the bitterness of the human bitter taste receptor TAS2R16 (Jeong, et al., 2023). The effects of only cellulase KN on GYP has not yet been reported. Moreover, the final products of naringinase depended on the microorganism's source (Zhu et al., 2017; Seong, et al., 2023). Zhu et al. (2017) showed that the naringinase from *Aspergillus oryzae*11250 could hydrolyze naringin to naringenin, while naringinase from *A. oryzae* NYO-2 hydrolyzed naringin to prunin and naringenin which had 13.1- and 300 times lower bitterness than naringin (Seong, et al., 2023). However, the effects of GYP matrix on naringinase to its physicochemical properties, the bitterness, and the anti-lipid accumulation of GYP were unclear. Therefore, to reduce the bitterness of GYP, 9 commercial enzymes and 2 naringinase from *A. oryzae* were screened for their ability to hydrolyze naringin and neohesperidin in GYP. The results of the hydrolysis of naringin and neohesperidin in GYP by 9 commercial enzymes and 2 naringinase from *A. oryzae* are shown in Fig. 1. HPLC analysis showed that the concentration of naringin and neohesperidin in GYP had decreased from  $10.92 \pm 0.66$  to  $1.09 \pm 0.09$  mg/g DW and from  $8.77 \pm 0.55$  to  $0.40 \pm 0.06$  mg/g DW, respectively (Fig. 1) after enzyme treatment. The content of naringin and neohesperidin in GYP decreased by 22.3–90.0 % and 21.3–95.4 %, respectively, by treating GYP with commercial enzymes. Of these enzymes, Pectinex XXL, Plantase CP, Plantase UF, Plantase PR, and Pectinex Ultra SP-L showed hydrolysis of less than 25 % of naringin and neohesperidin. In contrast, Rapidase Press, Rapidase Fiber, Cellulase KN, and Pectinex 100L hydrolyzed over 78 % of naringin and neohesperidin. In this study, we found that cellulase KN showed the most effective hydrolysis of naringin and neohesperidin of GYP by 90.02 % and 95.44 %, respectively. In comparison, naringinase from *A. oryzae* NYO-2 (naringinase NYO-2) diminished the content of naringin and neohesperidin by 87.8 % and 89.4 %, respectively (Fig. 1B), which was 5–10 % higher than naringinase from *A. oryzae* KCTC 6377. The decrease of naringin and neohesperidin of GYP using cellulase KN was possible due to cellulase KN from *A. niger* containing naringinase and cellulase that can hydrolyze naringin and neohesperidin (Jeong, et al., 2023). The results were consistent with a report by Jeong et al. (2023) that the content of naringin, narirutin, hesperidin, and neohesperidin of GYP was decreased, while naringenin and hesperetin of GYP were increased by combining cellulase KN with plantase UF and cellulase NY203 for treatment of GYP

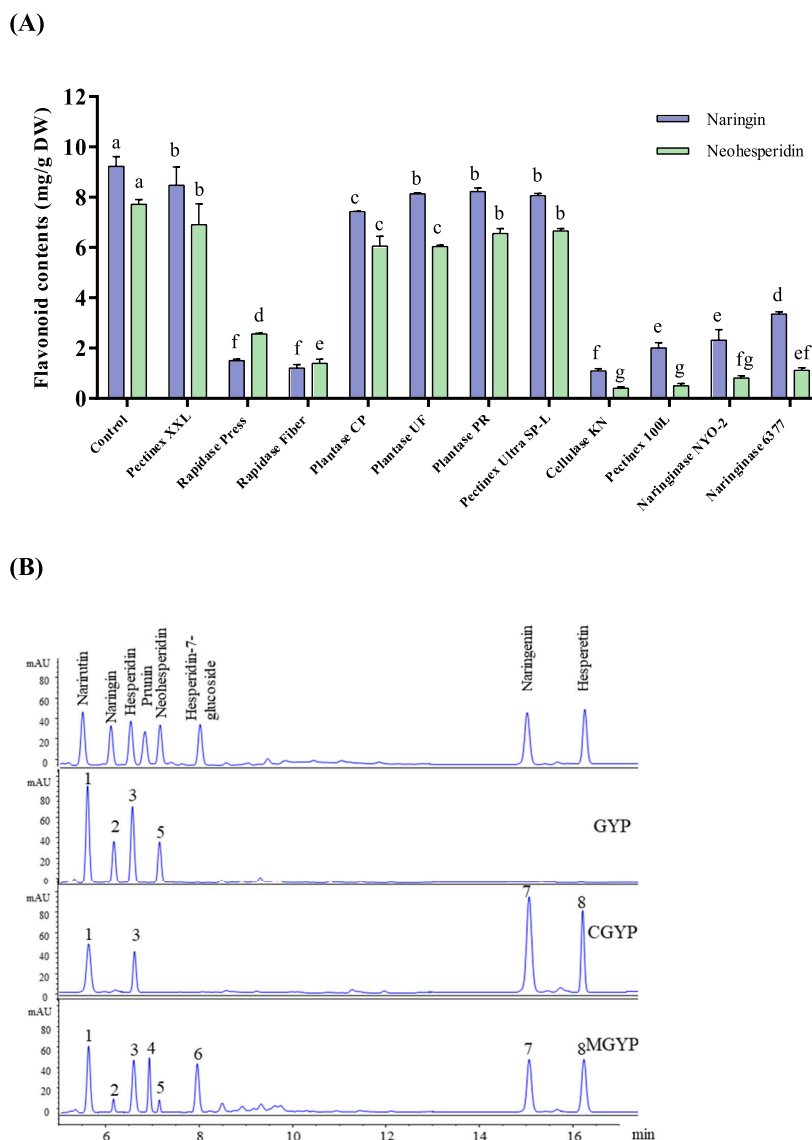


**Fig. 1.** The content of naringin and neohesperidin in GYP after treatment with different enzymes (A) and HPLC chromatogram analysis of GYP, CGYP, and MGYP (B). GYP, green yuzu powder; CGYP, treated green yuzu powder by Cellulase KN; MGYP, treated with green yuzu powder by naringinase NYO-2. Different lowercase letters represent the significant differences among fermentation time by Duncan's post-hoc test ( $p < 0.05$ ). 1, narirutin; 2, naringin; 3, hesperidin; 4, prunin; 5, neohesperidin; 6, hesperidin-7-glucoside; 7, naringenin; 8, hesperetin.

(Jeong, et al., 2023). Even though Cellulase KN is a food-grade enzyme commonly used to degrade cellulose, a major component of plant cell walls, it can hydrolyze phenolic compounds such as flavonoids and terpenoids, converting them into aglycones (Wang, Choi, Yu, Jin, & Im, 2016). However, studies are lacking on the enzyme treatment of citrus fruit, especially green yuzu, with *A. oryzae*-derived naringinase. The experiments conducted in this study contributed to filling this gap. However, HPLC analysis showed that naringenin, hesperetin, and hesperetin were detected in CGYP, whereas prunin, hesperidin-7-O-glucoside, naringenin, and hesperetin were found in MGYP. Therefore, along with Cellulase KN, naringinase from *A. oryzae* NYO-2 was selected for optimization and further study.

### 3.2. The effects of the concentration of enzyme and green yuzu powder, and reaction time on the hydrolysis of naringin and neohesperidin in green yuzu powder

The effects of enzyme concentration, GYP concentration, and reaction time on the hydrolysis of naringin and neohesperidin in GYP are shown in Fig. 2. The hydrolysis of naringin and neohesperidin was increased from 0 to 10.92 mg/g DW and 8.77 mg/g DW, respectively, when the enzyme concentration was increased from 0 % to 0.25 % (Fig. 2A). The highest hydrolysis of naringin and neohesperidin was achieved at 0.25 % enzyme for both Cellulase KN and naringinase NYO-2. At this concentration, naringin and neohesperidin were completely hydrolyzed by Cellulase KN and by 95.15 % and 90.08 %, respectively, by naringinase NYO-2. Even at a low concentration (0.1 %), Cellulase KN hydrolyzed 94.41 % naringin and 90.19 % neohesperidin. There was a non-significant difference between the hydrolysis of naringin and neohesperidin at 0.1 and 0.08 % enzyme.

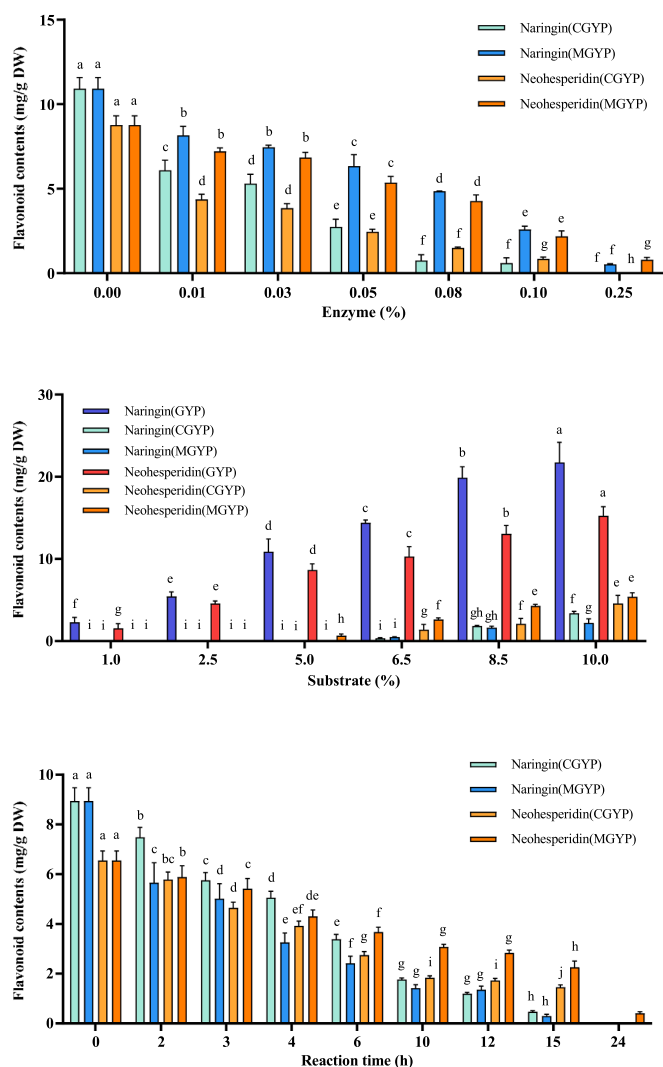


**Fig. 2.** Effects of enzyme concentration (A), GYP concentration (B), reaction time (C) on the hydrolysis of naringin and neohesperidin of GYP using Cellulase KN and naringinase NYO-2. GYP, green yuzu powder. Different lowercase letters represent the significant differences among fermentation time by Duncan's post-hoc test ( $p < 0.05$ ).

Regarding GYP concentration, naringin content increased from  $2.89 \pm 0.59$  mg/g DW at 1 % GYP to  $21.73 \pm 2.45$  mg/g DW at 10 % GYP, and neohesperidin was increased from  $1.56 \pm 0.55$  mg/g DW at 1 % GYP to  $15.26 \pm 1.10$  mg/g DW at 10 % YP (Fig. 2B). At 5 % GYP, naringin and neohesperidin were completely hydrolyzed by Cellulase KN, whereas 100 % naringin and 92.36 % neohesperidin were hydrolyzed by naringinase NYO-2 (Fig. 2B). Moreover, the hydrolysis of naringin and neohesperidin by Cellulase KN at 8.5 % GYP was 90.8 % and 83.91 %, respectively. Although naringinase NYO-2 had a similar hydrolysis rate to naringin at the same concentration (8.5 % GYP), the hydrolysis of neohesperidin by naringinase NYO-2 (67.2 %) was lower than that by Cellulase KN (83.91 %).

When investigating the effect of reaction time, the hydrolysis of naringin and neohesperidin increased when the reaction time was increased from 1 to 24 h (Fig. 2C). The hydrolysis of naringin was over 95 % at 15 h and complete at 24 h by both Cellulase KN and naringinase NYO-2. The hydrolysis of neohesperidin by Cellulase KN was 83.35 % at 15 h and complete at 24 h, whereas it was 74.23 % at 15 h and 95.32 % at 24 h by naringinase NYO-2.

### 3.3. Effects of enzyme treatment on the composition profiles of green yuzu powder

#### 3.3.1. Effects of enzyme treatment on the dietary fiber of green yuzu powder

Yuzu contains high dietary fiber, pectin, protein, and saccharide, contributing to its health-related benefits (Jeong, et al., 2023). Dietary fiber is classified into SDF and IDF. SDF can decrease the risk of cardiovascular disease, defense against colon cancer, and lowering the plasma cholesterol and glycemic response (Theuwissen & Mensink, 2008; Yu, Bei, Zhao, Li, & Cheng, 2018), while IDF exhibits the suppression of pancreatic lipase activity and boost the growth of intestinal flora (He, et al., 2015). Therefore, the effects of enzyme treatment on the dietary fiber of GYP were investigated, and the results are shown in Table 1. The TDF and SDF of GYP were increased from  $49.45 \pm 1.32$  % to  $54.19 \pm 1.63$  % and from  $18.21 \pm 1.33$  % to  $27.52 \pm 0.59$  %, respectively, by treating with enzyme (Table 1). In contrast, the IDF of both CGYP and MGYP decreased from  $31.24 \pm 1.02$  % to  $25.64 \pm 0.58$  % (Table 1). Although there was no significant difference in TDF and SDF between CGYP and MGYP, there was a significant difference in the IDF, which was 1.14 % lower in MGYP than in CGYP. The TDF and SDF of enzyme-treated GYP were increased by 1.10- and 1.5-fold compared to non-treated GYP, while the IDF content was decreased by 1.22-fold. These results were consistent with previous studies of modified cumin dietary fiber by cellulase or cellulase and laccase (Ma & Mu, 2016) and carrot pomace insoluble dietary fiber by complex enzymes composed of cellulase and xylanase (Yu, Bei, Zhao, Li, & Cheng, 2018). In contrast, Jeong et al. (2023) revealed that the IDF and SDF of GYP decreased using complex enzymes, including cellulase KN, plantase UF, and cellulase NY203. The decreasing IDF content in enzyme-treated GYP was possibly caused by the degradation of IDF by enzymes such as crystalline cellulose to amorphous cellulose that improved the physicochemical of GYP (Liu, Zhang, Yi, Quan, & Lin, 2021).

**Table 1**

The composition profiles of green yuzu powder (GYP) treated with Cellulase KN and naringinase NYO-2 enzymes.

	Compound	GYP	CGYP	MGYP
Dietary fiber content (%)	TDF	$49.45 \pm 1.32^b$	$54.19 \pm 1.63^a$	$52.16 \pm 3.99^a$
	SDF	$18.21 \pm 1.33^b$	$26.41 \pm 1.08^a$	$27.52 \pm 0.59^a$
	IDF	$31.24 \pm 1.02^a$	$26.78 \pm 0.45^b$	$25.64 \pm 0.58^c$
Dietary fiber composition (mg/g DW)	Cellulose	$67.80 \pm 0.85^a$	$33.85 \pm 5.09^b$	$34.88 \pm 4.03^b$
	Hemicellulose	$56.00 \pm 6.76^a$	$46.15 \pm 1.84^b$	$39.33 \pm 3.80^c$
	Lignin	$70.40 \pm 3.96^a$	$35.80 \pm 7.63^b$	$34.60 \pm 2.59^b$
	Pectin	$188.84 \pm 5.81^a$	$163.50 \pm 3.19^c$	$166.08 \pm 6.38^b$
Free sugars (mg/g DW)	Rhamnose	$0.00 \pm 0.00^c$	$3.60 \pm 0.17^a$	$2.18 \pm 0.16^b$
	Xylose	$0.03 \pm 0.00^c$	$0.29 \pm 0.07^b$	$0.42 \pm 0.09^a$
	Fructose	$2.91 \pm 0.63^c$	$4.47 \pm 0.63^a$	$3.48 \pm 0.55^b$
	Glucose	$2.42 \pm 0.55^c$	$4.22 \pm 0.59^a$	$3.31 \pm 0.49^b$
	Sucrose	$6.83 \pm 0.42^a$	$4.02 \pm 0.23^b$	$4.22 \pm 0.25^b$
	Galacturonic acid	$0.09 \pm 0.00^c$	$0.36 \pm 0.08^a$	$0.26 \pm 0.07^b$

Different lowercase letters represent the significant differences among fermentation time by Duncan's post-hoc test ( $p < 0.05$ ).

### 3.3.2. Effects of enzyme treatment on the content of cellulose, hemicellulose, lignin, and pectin in green yuzu powder

Cellulose, insoluble hemicellulose, and lignin are components of IDF, while pectic substance and soluble hemicellulose are the main components of SDF. Therefore, the cellulose, hemicellulose, lignin, and pectin in GYP, CGYP, and MGYP were analyzed (Table 1). Cellulose, hemicellulose, lignin, and pectin content in CGYP decreased 2.0-, 1.21-, 1.97, and 1.15-fold lower than GYP (Table 1). In addition, the cellulose, hemicellulose, lignin, and pectin content in MGYP reduced by 1.94-, 1.42-, 2.02-, and 1.14-fold compared to the control (Table 1). Even though cellulose and lignin contents were non-significant differences between CGYP and MGYP, there were significant differences in hemicellulose and pectin content of CGYP and MGYP. Especially the hemicellulose content in MGYP was 14.78 % lower than that of CGYP.

### 3.3.3. Effects of enzyme treatment on free sugars in green yuzu powder

The free sugars, including rhamnose, xylose, fructose, glucose, sucrose, and galacturonic acid in GYP, CGYP, and MGYP, were analyzed using HPLC, and the results are shown in Table 1. In addition to similarities in dietary fiber contents and dietary fiber composition, we observed differences in monosaccharide contents among GYP, CGYP, and MGYP. The free sugars of GYP were increased from 0 to  $3.60 \pm 0.17$  mg/g DW for rhamnose, from 0.03 mg/g DW to  $0.42 \pm 0.09$  mg/g DW for xylose, from  $2.91 \pm 0.63$  mg/g DW to  $4.47 \pm 0.63$  mg/g DW for fructose, and from  $2.42 \pm 0.55$  mg/g DW to  $4.22 \pm 0.59$  mg/g DW for glucose by enzyme treatment. Additionally, the contents of rhamnose, fructose, glucose, and galacturonic acid in CGYP were 1.65-, 1.28-, 1.28-, and 1.39-fold higher than those of MGYP, respectively. In contrast, xylose in MGYP was 1.45-fold higher compared to CGYP. In this study, we observed that cellulose, hemicellulose, lignin, and pectin content in CGYP and MGYP were decreased compared to those in GYP (Table 1), while free sugars, including rhamnose, xylose, fructose, glucose, and galacturonic acid of GYP was increased following enzyme treatments (Table 1). Interestingly, rhamnose that was not detected in GYP, was detected as  $3.60 \pm 0.17$  mg/g DW in CGYP and  $2.18 \pm 0.16$  mg/g DW in MGYP, which was consistent with the results found in the hydrolysis of naringin and neohesperidin by naringinase (Seong, et al., 2023). These results were in line with the outcomes of previous research conducted on

the application of enzymatic treatment to different types of fruit peels and carrot pomace (Ma, Ren, Diao, Chen, Qiao, & Liu, 2016; Song, Qi, Liao, & Yang, 2021; Zheng & Li, 2018). These enzymes can break down the glycosidic linkages in lignin, cellulose, hemicellulose, which results in changes in TDF, SDF, IDF, cellulose, hemicellulose, lignin, pectin, and monosaccharides (Cheng, Zhang, Hong, Li, Li, & Gu, 2017). Especially, the SDF content of MGYP was 1.1 % higher compared to CGYP, and the IDF content was 4.06 % lower. This can be seen in conjunction with the changes in the contents of cellulose, hemicellulose, lignin, and pectin. Contreras-Esquivel, Voget, Vita, Espinoza-Perez, and Renard (2006) reported that polygalacturonase obtained from *Aspergillus* sp. can enzymatically break down the pectin that makes up the cell wall, resulting in the release of rhamnose, xylose, and galactose. In another study, Ma et al. (2016) found that SDF, uronic acid, and monosaccharides increased when carrot pomace was treated with laccase and cellulase under high hydrostatic pressure (Ma, Ren, Diao, Chen, Qiao, & Liu, 2016). Therefore, these results indicate that the composition of dietary fiber is intricately linked to free sugar content, and changes in these components can affect the physical and functional properties of the fibers.

### 3.4. Effects of enzyme treatment on the structure of green yuzu powder

#### 3.4.1. FE-SEM observation of enzyme treated green yuzu powder

The GYP, CGYP, and MGYP morphologies are shown in Fig. 3A. The surface of GYP appeared devoid of perforations and exhibited a smooth appearance. In comparison, the CGYP and MGYP structures were noticeably more porous and had several apparent holes and cracks, which may have been caused by the degradation of the ordered fibre network (Table 1).

#### 3.4.2. FT-IR analysis

The FT-IR spectroscopy revealed that GYP, CGYP, and MGYP had similar characteristic spectra (Fig. 3B). The peak observed at  $3411 \text{ cm}^{-1}$  was associated with intramolecular hydrogen bonding of -OH groups in the cellulose and hemicellulose crystalline region (Cui, Phillips, Blackwell, & Nikiforuk, 2007; Song, Qi, Liao, & Yang, 2021). Compared to GYP, the absorption band and peak intensity of CGYP and MGYP were

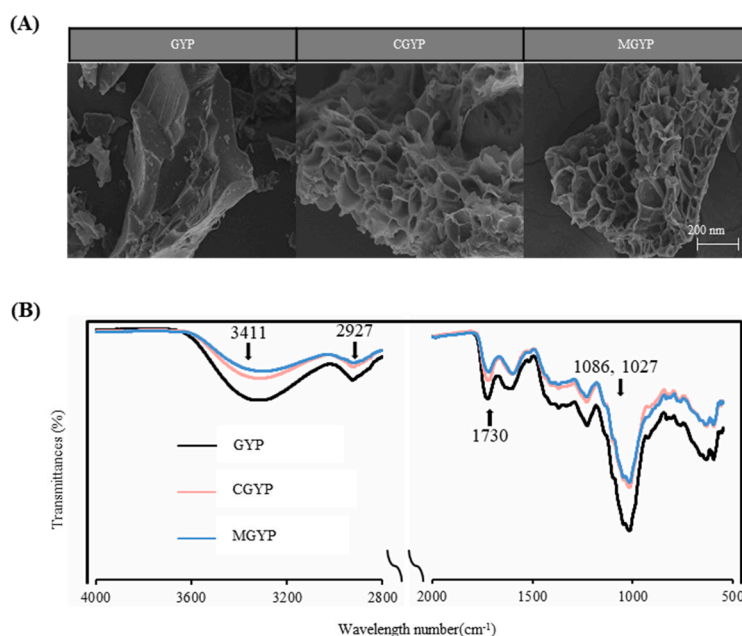


**Fig. 3.** Field emission scanning electron microscopy (A) and Fourier-transform infrared spectra (B) of GYP, CGYP, and MGYP. GYP, green yuzu powder; CGYP, treated green yuzu powder by Cellulase KN; MGYP, treated with green yuzu powder by naringinase NYO-2.

decreased, suggesting the destruction of hydrogen bonds in hemicellulose and cellulose. The C—H stretching vibrations of polysaccharides were detected at  $2927\text{ cm}^{-1}$  in all citrus fibers, and the reduced absorption intensity at this frequency in modified citrus fibers indicated a potential decrease in polysaccharide content and disruption of hydrogen bonding between —OH groups in the cellulose crystalline structure (Song, Qi, Liao, & Yang, 2021). The absorbance peak around  $1730\text{ cm}^{-1}$ , indicative of uronic acid from pectin, was weaker in CGYP and MGYP compared to GYP, suggesting possible removal and degradation of pectin by enzyme treatment (Zhang, Qi, Zeng, Huang, & Yang, 2020) (Table 1). Different types of polysaccharides can be distinguished in the “fingerprint” range of  $800$  to  $1300\text{ cm}^{-1}$ , and the peak intensity at  $1086\text{ cm}^{-1}$  in SDF may be attributed to mixed vibrations of C—O—C and C—O—H (Liu, et al., 2022; Ma et al., 2023). The peak observed around  $1029\text{ cm}^{-1}$  is attributed to the vibration of methoxy groups in lignin and hemicellulose that contain carbon-oxide bond (C—O) (Sain & Panthapulakkal, 2006). Almost all characteristic peaks’ cellulose, hemicellulose, and lignin intensity decreased in CGYP, and MGYP compared to those of GYP. Enzyme treatment’s removal of cellulose, hemicellulose, and lignin may raise the surface roughness and enhance the GYP’s WHC and SWC (Zhang, Qi, Zeng, Huang, & Yang, 2020).

### 3.5. Physicochemical characterization of enzyme treated green yuzu powder

#### 3.5.1. Effects of enzyme treatment on particle size of green yuzu powder

The particle size distribution of GYP, CGYP, and MGYP are shown in Table 2. The mean particle size of GYP was  $1184.31 \pm 61.4\text{ nm}$ . Its size was reduced to  $530.37 \pm 19.5\text{ nm}$  and  $340.18 \pm 41.5\text{ nm}$  after Cellulase and naringinase NYO-2 treatment, respectively (Fig. S1, Table 2). The polydispersity index (PDI) was used to evaluate the particle size dispersion. The PDI of GYP was  $0.64 \pm 0.04$ , indicating a broad particle size distribution. In contrast, the PDI of CGYP and MGYP was  $0.34 \pm 0.01$  and  $0.26 \pm 0.01$ , respectively, indicating high particle homogeneity (Jiang, et al., 2022). The zeta potential is used to measure of the stability of dispersed systems. Júnior and Baldo (2014) reported that a zeta potential absolute value of  $30\text{ mV}$  indicates a stable suspension. Herein, we observed that after enzymatic treatment, the zeta potential of GYP increased, indicating improved stability of GYP (Song, Qi, Liao, &

**Table 2**

Physicochemical properties and product stability of enzyme-treated green yuzu powders (CGYP and MGYP).

	GYP	CGYP	MGYP
Diameter (nm)	$1184.31 \pm 61.4^a$	$530.37 \pm 19.5^b$	$340.18 \pm 41.5^c$
Polydispersity index (PDI)	$0.64 \pm 0.04^a$	$0.34 \pm 0.01^b$	$0.26 \pm 0.01^c$
Zeta potential (mV)	$-21.31 \pm 1.27^a$	$-37.49 \pm 2.25^c$	$-33.96 \pm 1.45^b$
Water holding capacity (g/g)	$5.18 \pm 0.03^b$	$5.89 \pm 0.08^a$	$6.23 \pm 0.15^a$
Oil holding capacity (g/g)	$3.60 \pm 0.01^c$	$6.25 \pm 0.35^a$	$5.85 \pm 0.07^b$
Solubility (%)	$20.99 \pm 1.41^c$	$71.99 \pm 4.24^{ab}$	$77.51 \pm 7.78^a$
Water swelling capacity (mL/g)	$9.50 \pm 0.71^c$	$10.02 \pm 0.85^b$	$11.50 \pm 1.12^a$
Soluble solids (°Brix)	$2.80 \pm 0.00^c$	$3.43 \pm 0.06^a$	$3.23 \pm 0.06^b$
Hunter's color value			
$L^*$	$87.305 \pm 0.010^a$	$82.366 \pm 0.004^b$	$79.999 \pm 0.002^c$
$a^*$	$-3.847 \pm 0.005^c$	$-1.081 \pm 0.003^b$	$0.527 \pm 0.005^a$
$b^*$	$26.884 \pm 0.005^c$	$28.891 \pm 0.008^b$	$32.139 \pm 0.002^a$
$\Delta E^*$	$90.485 \pm 0.011^a$	$86.358 \pm 0.006^b$	$85.297 \pm 0.003^c$

Different lowercase letters represent the significant differences among fermentation time by Duncan's post-hoc test ( $p < 0.05$ ).

Yang, 2021).

#### 3.5.2. Effects of enzyme treatment on water holding capacity, water swelling capacity, solubility, and oil holding capacity of green yuzu powder

As shown in Table 2, the WHC, WSC, and solubility of GYP were increased after enzyme treatment. The WHC of GYP was increased by 13.7 % by Cellulase KN treatment and 20.27 % by naringinase NYO-2 treatment. However, the differences in WHC between CGYP and MGYP were non-significant. MGYP exhibited the highest WSC value ( $11.50 \pm 1.12\text{ g/g}$ ), followed by CGYP ( $10.02 \pm 0.85\text{ g/g}$ ). WSC increased by 5.47 % for CGYP and 21.05 % for MGYP compared to GYP (Table 2). The solubility was increased from  $20.99 \pm 1.41\%$  for GYP to  $71.99 \pm 4.24\%$  for CGYP and  $77.51 \pm 7.78\%$  for MGYP (Table 2), corresponding to 3.43- and 3.69-fold higher solubility, respectively. The OHC value was increased from  $3.6 \pm 0.01\text{ g/g}$  for GYP to  $6.25 \pm 0.35\text{ g/g}$  for CGYP and  $5.85 \pm 0.07\text{ g/g}$  for MGYP (Table 2), corresponding to increases of 73.61 % and 62.5 %, respectively, compared to GYP, which was higher than that obtained from complex enzymes, including cellulase KN, plantase UF, and cellulase NY203 (1.15-fold) (Jeong, et al., 2023). Chau, Wang, & Wen (2007) reported that the increasing of soluble dietary fiber could increase hydrophilic groups, water-binding sites, and surface area and decrease particle sizes and bulk density, that were come up with higher WHC, WSC, and solubility, and hold more oil. In this study, we found that the cellular structure of GYP was modified via SEM images. CGYP and MGYP contained more porosity (Fig. 3A), making it easy to entrap water molecules within the fibre network that may contribute to increasing WHC, WSC and solubility (Liu, et al., 2016; Peerajit, Chiewchan, & Devahastin, 2012). The particle size of CGYP and MGYP was smaller than GYP, which provided a larger surface area (Hahn, Nöbel, Maisch, Rösingh, Weiss, & Hinrichs, 2015). Moreover, the decrease of GYP's cellulose, hemicellulose, and lignin content after enzyme treatment due to hydrolyzing of glycosidic linkages between hemicellulose and cellulose or lignin caused the change of GYP structure and expose more hydrophilic groups, which affects the increase of solubility, WHC, and WSC values (Song, Qi, Liao, & Yang, 2021).

#### 3.5.3. Soluble solid and Hunter's color value of enzyme-treated green yuzu powder

There was an increase in the soluble solids content of GYP ( $2.80^\circ\text{Brix}$ ) after enzyme treatment for both CGYP ( $3.43^\circ\text{Brix}$ ) and MYP ( $3.23^\circ\text{Brix}$ ), which could be attributed to the release of free sugars from dietary fiber and flavonoids (Table 2). Furthermore, compared to YP, the enzymatic treatment resulted in a decrease in a decrease in brightness ( $L^*$ ) and an increase in both the redness ( $a^*$ ) and yellowness ( $b^*$ ) values. These findings suggest that enzymatic treatment can improve citrus fibers' physical characteristics and properties.

#### 3.6. Effects of enzyme treatment on the bitterness of green yuzu powder

In this study, the electronic tongue was employed to measure the samples' overall taste. Each sensor's sensitivity was depicted as a radar plot ranging from 0 to 10 (Fig. 4A). In comparison to GYP, the bitterness and sourness of CGYP and MGYP were decreased, while the sweetness, umami, and saltiness of CGYP and MGYP were increased (Fig. 4A). The bitterness of GYP was reduced by 37.93 % and 55.17 % by Cellulase KN and naringinase NYO-2, respectively. Naringin and neohesperidin are known as the bitter compounds in GYP (Nam, et al., 2021), while the bitterness of naringin and neohesperidin was reduced when their glycoside residues were removed (Seong et al., 2023). This finding was consistent with our previous study that the bitterness of GYP was reduced 50 % by treatment with complex enzymes (Jeong, et al., 2023). Principal component analysis (PCA) (Fig. 4B) was conducted to analyze the relative difference between GYP and enzyme-treated GYP. PCA analysis facilitates the segregation of samples onto a bi-dimensional graph, relying on the samples' two leading principal components (PC1

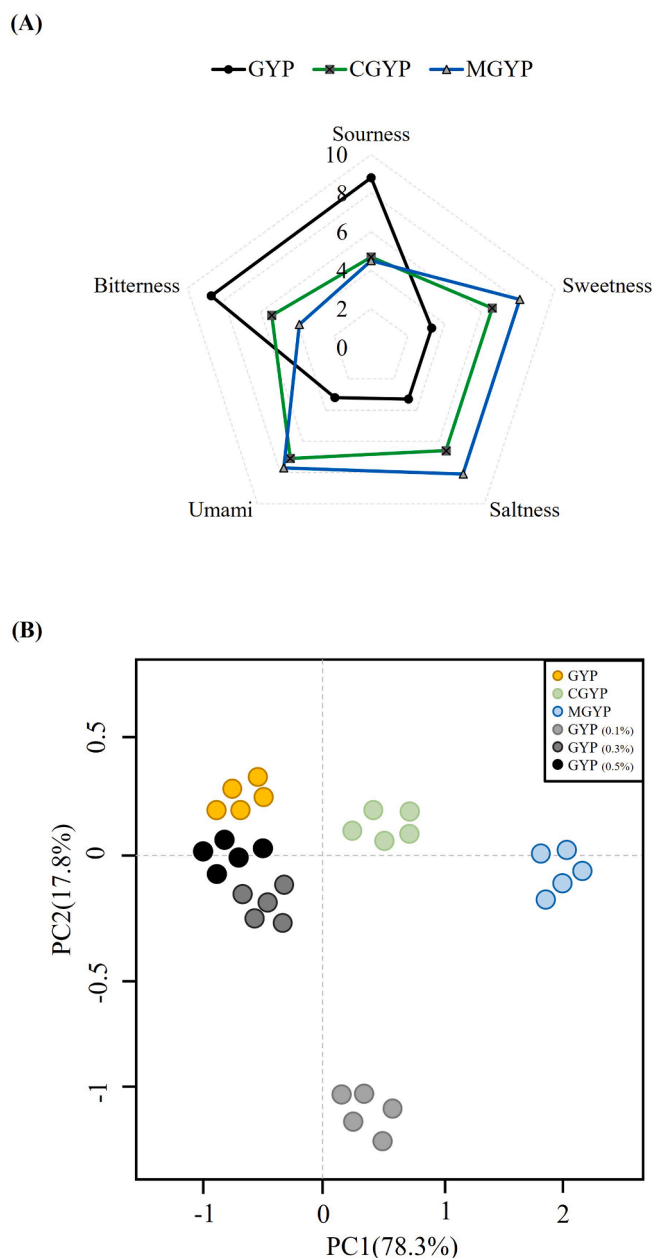


**Fig. 4.** Radar plot (A) and principal component analysis scores plot (B) of the electronic tongue analysis of GYP, CGYP, and MGYP. GYP, green yuzu powder; CGYP, treated green yuzu powder by Cellulase KN; MGYP, treated with green yuzu powder by naringinase NYO-2.

and PC2) of the sample. The bi-dimensional PCA plot describes 96.1 % of the total variations, with PC1 and PC2 accounting for 78.3 % and 17.8 % of the total variances, respectively. With increasing amounts of naringin and neohesperidin in GYP, the samples were observed to move in a negative direction on the PC1 axis and a positive direction on the PC2 axis. Conversely, when the amounts of these compounds decreased, the samples moved in a positive direction on the PC1 axis and a negative direction on the PC2 axis. In the order of GYP, CGYP, and MGYP, the samples moved toward the positive axis of PC1 and negative axes of PC2.

### 3.7. Effects of enzyme-treated green yuzu powders on the free glycerol content, fatty acid synthase content, and lipid accumulation in 3T3-L1 cells

In this study, we found that the flavonoid composition and content of

GYP varied according to enzyme treatment. Kim et al. (2012) reported that *Citrus aurantium* flavonoids displayed the suppression of lipid accumulation in 3T3-L1 cells, reduced the triglyceride content, and increased the glycerol released in the medium as the dose-dependent manner, which inhibits adipogenesis by down-regulating of peroxisome proliferating-activated receptor-gamma (PPAR $\gamma$ ) and CCAAT-enhancer binding protein-alpha (C/EBP $\alpha$ ) as well as by down-regulated fatty acid synthase genes. Therefore, the cell viability, anti-lipid accumulation effects, free glycerol release, and fatty acid synthase (FAS) contents in mouse 3T3-L1 cells of GYP, CGYP, and MGYP were investigated in this study.

#### 3.7.1. Mouse 3T3-L1 cell viability

The effects of GYP, CGYP, and MGYP on 3T3-L1 preadipocyte and adipocyte viability are shown in Fig. 5A, B. Although treatment with GYP at 250  $\mu$ g/mL resulted in more than 80 % viability of both pre-adipocytes and adipocytes, less than 80 % preadipocyte viability following treatment with CGYP and MGYP at 100  $\mu$ g/mL, respectively (Fig. 5A). In contrast, treatment with CGYP and MGYP showed more than 90 % for adipocytes viability (Fig. 5B). Therefore, GYP, CGYP, and MGYP at 10, 20, and 40  $\mu$ g/mL were selected for further experiments.

#### 3.7.2. Inhibitory effects of enzyme-treated green yuzu powder on the lipid accumulation in mouse 3T3-L1 cells

The formation of lipid droplets in mouse 3T3-L1 cells treated by GYP, CGYP, and MGYP after Oil-red O staining under the microscope was shown in Fig. 5C. Microscopic observations revealed a reduction of lipid droplets, a maker of lipid accumulation in 3T3-L1 cells treated by CGYP and MGYP compared to GYP. Fig. 5D showed the reduction of lipid accumulation by treatment with GYP, CGYP, and MGYP in dose-dependent manner. Although the inhibitory activity against lipid accumulation in mouse 3T3-L1 cells at 10  $\mu$ g/mL was no significant difference between GYP and CGYP, CGYP expressed 1.42- and 1.22-fold higher inhibitory activity against lipid accumulation in mouse 3T3-L1 cells at 20 and 40  $\mu$ g/mL than that of GYP. Moreover, MGYP showed 2.50-, 1.54-, and 1.38-fold higher inhibitory activity against lipid accumulation in mouse 3T3-L1 cells at 10, 20, and 40  $\mu$ g/mL compared to the control, respectively. Furthermore, MGYP expressed higher inhibitory activity against lipid accumulation in mouse 3T3-L1 cells compared to CGYP. Cellulase KN and naringinase NYO-2 hydrolyzed naringin and neohesperidin in GYP to their aglycones. Sharma, Adhikari, Kim, Oh, Oak, & Yi (2019) reported that these aglycones are more efficacious in mitigating lipid accumulation than glycoside compounds. Therefore, aglycones in CGYP and MGYP contributed to their higher inhibitory activity against lipid accumulation in mouse 3T3-L1 cells compared to YP.

#### 3.7.3. Effects of enzyme-treated green yuzu powder on the released free glycerol in mouse 3T3-L1 cells

The lipolysis capabilities of GYP, CGYP, and MGYP were evaluated by measuring the amount of glycerol released into the medium of the treated mouse 3T3-L1 cells due to the breakdown of triglycerides into fatty acids and glycerol (Fig. 5E). GYP, CGYP, and MGYP showed a greater release of free glycerol compared to the control. The free glycerol released in mouse 3T3-L1 cells treated with MGYP and CGYP at 40  $\mu$ g/mL was 0.123 and 0.130 mM, respectively, which was an increase of approximately 25 % compared to the control. The concentration-dependent increase in free glycerol observed with GYP, MGYP, and CGYP treatments is consistent with the findings of a study conducted by Kim (Kim, et al., 2012), which investigated the effect of citrus flavonoids on lipolysis in 3T3-L1 cells.

#### 3.7.4. Inhibitory effects of enzyme-treated green yuzu powder on the fatty acid synthase (FAS) contents in mouse 3T3-L1 cells

FAS is a lipogenic enzyme that facilitates triglyceride synthesis and cytoplasmic storage and is associated with lipid accumulation during

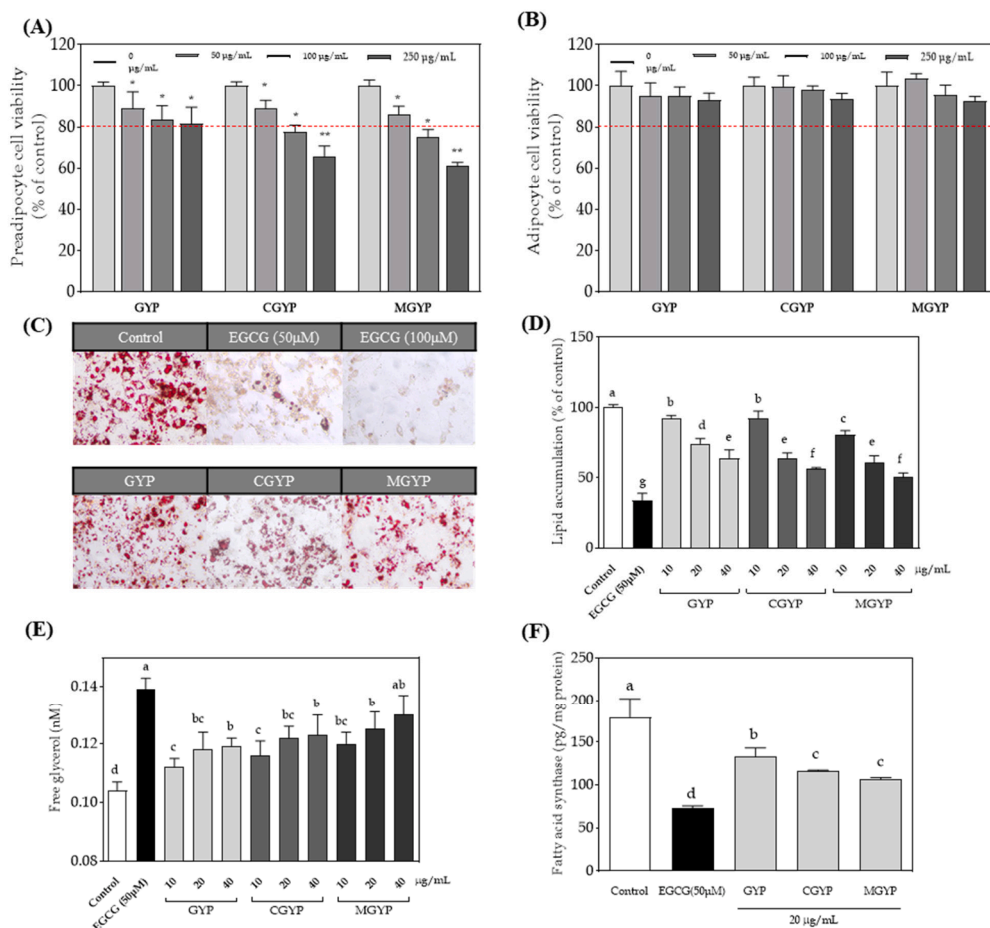


**Fig. 5.** Preadipocyte cell viability (A), adipocyte cell viability (B), lipid droplets accumulation by oil red O staining observed under microscope (C), lipid accumulation (D), glycerol release (D), and fatty acid synthase (F) in mouse 3T3-L1 cells treated by GYP, CGYP, and MGYP. GYP, green yuzu powder; CGYP, treated green yuzu powder by Cellulase KN; MGYP, treated with green yuzu powder by naringinase NYO-2. Different lowercase letters represent the significant differences among fermentation time by Duncan's *t* post-hoc test ( $p < 0.05$ ).

adipogenesis (Poudel, et al., 2015). To measure FAS, GYP, CGYP, and MGYP were treated during adipocyte differentiation. GYP, CGYP, and MGYP all showed a decrease in FAS compared to the control. There was no significant difference between the FAS levels found in cells treated with CGYP and MGYP, which were 116.16 and 106.29 pg/mg protein, respectively. Poudel (Poudel, et al., 2015) found that luteolin, an aglycone of isoorientin, effectively inhibited FAS production, which is consistent with the results obtained in the present study. The flavonoids were found to effectively decrease FAS not only in 3T3-L1 cells but also in animal experiments (Wu, Yang, Chan, Chung, Ou, & Wang, 2010). Therefore, the results suggested that the different flavonoid composition and contents caused the difference in inhibiting lipid accumulation, free glycerol release, and fatty acid synthase contents among GYP, CGYP, and MGYP-treated 3T3-L1 cells.

### 3.8. Multivariate analysis

In this study, the correlation between flavonoids, free sugars, physicochemical properties, and functional properties of GYP were studied. The results are shown in Fig. 6A. From the Fig. 6A, WHC, OHC, and WSC had strong negative correlations with dietary fiber components such as cellulose, hemicellulose, and lignin but positive correlations with free sugars like rhamnose, xylose, glucose, fructose, and galacturonic acid. These findings were in line with previous studies that investigated the changes in dietary fiber composition due to enzyme treatment (Cheng, Zhang, Hong, Li, Li, & Gu, 2017). Several studies have reported that

flavonoids have positive effects on the body's bioactivity and that they also inhibit adipogenesis in 3T3-L1 cells (Sharma, Adhikari, Kim, Oh, Oak, & Yi, 2019). Bitterness showed strong positive correlations with naringin and neohesperidin, but negative correlations with flavonoids produced by the enzymatic reaction (prunin, naringenin, hesperetin-7-O-glucoside and hesperetin) and free sugars (rhamnose and glucose). These findings were consistent with a previous study that measured the bitterness of non-glycosylated flavonoids from yuzu (Seong, et al., 2023). The results of the correlation analysis suggest that the substances removed and produced during the enzymatic reaction and the changes in physicochemical properties are closely related to each other.

Furthermore, the variation between enzyme treatment and all the characteristic features of GYP were investigated by using PCA analysis. The results are shown in Fig. 6B. As depicted in Fig. 6B, the two main components of the principal component analysis (PCA), PC1 and PC2, explained 88.8 % of the overall variation in the data, indicating a noteworthy association between the enzyme treatment and all the characteristic features of GYP. The loading plot demonstrated that PC1 accounted for 70.9 % of the total variance, whereas PC2 explained only 16.9 % of the overall variability. The significant factors that contributed to the formation of PC1 included bitterness, flavonoids (naringin, neohesperidin, naringenin, and hesperetin), dietary fiber (cellulose, hemicellulose, and lignin), and physicochemical properties (OHC and solubility). The major factors influencing PC2 were xylose, fructose, IDF, and glucose, mainly representing dietary fiber and free sugar content. The study found that enzyme treatment significantly impacted GYP's

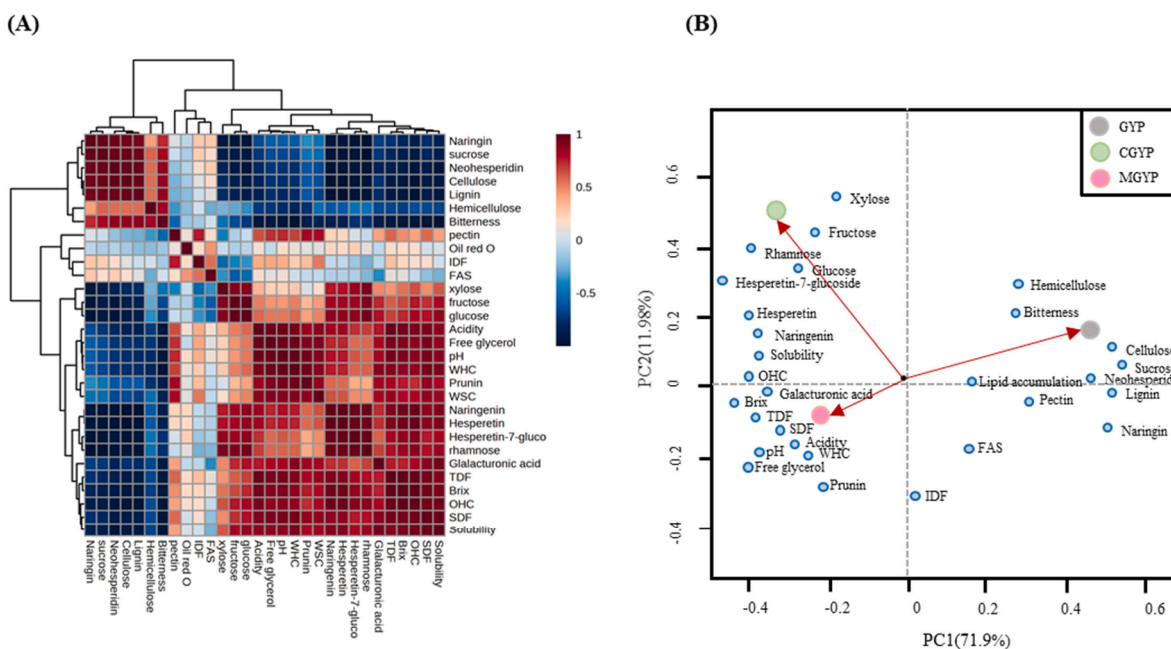


**Fig. 6.** Correlation of different in physicochemical properties and composition profiles (A) and principal component analysis (B) of GYP, CGYP, and MGYP. GYP, green yuzu powder; CGYP, treated green yuzu powder by Cellulase KN; MGYP, treated with green yuzu powder by naringinase NYO-2.

bioactive compounds and composition. These results are consistent with previous studies, indicating that enzyme treatment can alter both the dietary fiber content and physical and functional properties of food (Cheng, Zhang, Hong, Li, Li, & Gu, 2017; Song, Qi, Liao, & Yang, 2021; Zhang, Qi, Zeng, Huang, & Yang, 2020). Compared to GYP, CGYP, and MGYP are more like free glycerol and further away from FAS and lipid accumulation, indicating that they effectively inhibit lipogenesis and lipolysis. The correlation analysis and PCA results indicated that the commercial and microbial enzymes used in this experiment significantly impacted GYP's composition, physicochemical properties, and bioactive constituents.

#### 4. Conclusions

In this study, Cellulase KN and naringinase NYO-2 were screened from 9 commercials and 2 naringinase for their ability to hydrolyze naringin and neohesperidin in GYP. The optimal conditions for greater than 80 % hydrolysis of naringin and neohesperidin were achieved at 0.1 % Cellulase KN and 6.5 % GYP for 12 h reaction, whereas it was 0.25 % naringinase NYO-2 and 6.5 % GYP for 24 h reaction. The physicochemical properties and dietary fiber contents of CGYP and MGYP were also evaluated, and they were found to have an increased amount of total dietary fiber and soluble dietary fiber, while insoluble dietary fiber decreased compared to GYP. In addition, WHC, OHC, and WSC increased, improving dietary fiber properties. CGYP and MGYP showed significantly lower lipid accumulation and higher lipolysis capability compared to GYP, and all three samples exhibited decreased FAS content in 3T3-L1 cells compared to the control. The correlation and PCA analysis revealed that the enzymatic treatment reduced GYP's bitter taste and improved its physicochemical properties due to changes in the composition of sugars and dietary fiber. Based on these findings, CGYP and MGYP could be used as functional food ingredients.

#### CRedit authorship contribution statement

**Hyeon-Jun Seong:** Writing – original draft, Visualization, Methodology, Formal analysis, Data curation. **Hayeong Kim:** Writing – review & editing, Validation, Methodology, Formal analysis. **Jeong-Yong Cho:**

Validation, Formal analysis. **Kwang-Yeol Yang:** Writing – review & editing, Resources, Investigation. **Seung-Hee Nam:** Writing – review & editing, Supervision, Project administration, Funding acquisition, Conceptualization.

#### Declaration of competing interest

The authors declare that they have no known competing financial interests or personal relationships that could have appeared to influence the work reported in this paper.

#### Data availability

Data will be made available on request.

#### Acknowledgments

This study was financially supported by productivity of agricultural products for export and development of postharvest management technology of Rural Development Administration (Project No. RS-2023-00236699) and partially by agriculture science and technology development program of Rural Development Administration.

#### Appendix A. Supplementary data

Supplementary data to this article can be found online at <https://doi.org/10.1016/j.fochx.2024.101329>.

#### References

- Benavente-Garcia, O., & Castillo, J. (2008). Update on uses and properties of citrus flavonoids: New findings in anticancer, cardiovascular, and anti-inflammatory activity. *Journal Agricultural and Food Chemistry*, 56(15), 6185–6205.
- Chau, C. F., Wang, Y. T., & Wen, Y. L. (2007). Different micronization methods significantly improve the functionality of carrot insoluble fibre. *Food Chemistry*, 100(4), 1402–1408.
- Cheng, L., Zhang, X. M., Hong, Y., Li, Z. F., Li, C. M., & Gu, Z. B. (2017). Characterisation of physicochemical and functional properties of soluble dietary fibre from potato pulp obtained by enzyme-assisted extraction. *International Journal of Biological Macromolecules*, 101, 1004–1011.

- Contreras-Esquivel, J. C., Voget, C. E., Vita, C. E., Espinoza-Perez, J. D., & Renard, C. M. G. C. (2006). Enzymatic extraction of lemon pectin by endo-polygalacturonase from *Aspergillus niger*. *Food Science and Biotechnology*, 15, 163–167.
- Cui, S. W., Phillips, G. O., Blackwell, B., & Nikiforuk, J. (2007). Characterisation and properties of *Acacia senegal* (L) Willd. var. *senegal* with enhanced (acacia (sen) SUPERGUMTM): Part 4. spectroscopic characterisation of *Acacia senegal* var. *senegal* and *Acacia* (sen) SUPERGUMTM arabic. *Food Hydrocolloids*, 21(3), 347–352.
- Hahn, C., Nöbel, S., Maisch, R., Rösingh, W., Weiss, J., & Hinrichs, J. (2015). Adjusting rheological properties of concentrated microgel suspensions by particle size distribution. *Food Hydrocolloids*, 49, 183–191.
- He, B., Nohara, K., Ajami, N. J., Michalek, R. D., Tian, X., Wong, M., Losee-Olson, S. H., Petrosino, J. F., Yoo, S. H., Shimomura, K., & Chen, Z. (2015). Transmissible microbial and metabolomic remodeling by soluble dietary fiber improves metabolic homeostasis. *Sci Rep*, 5, 10604.
- Jeong, H., Das, P. R., Kim, H., Im, A. E., Lee, B. B., Yang, K. Y., & Nam, S. H. (2023). A combination of commercial and traditional food-source-derived enzymatic treatment acts as a potential tool to produce functional yuzu (*Citrus junos*). *Food Chemistry-X*, 20, Article 100918.
- Jiang, L. W., Xia, N., Wang, F. H., Xie, C. C., Ye, R., Tang, H. J., Zhang, H. J., & Liu, Y. Z. (2022). Preparation and characterization of curcumin/beta-cyclodextrin nanoparticles by nanoprecipitation to improve the stability and bioavailability of curcumin. *Lwt-Food Science and Technology*, 171, Article 114149.
- Júnior, J. A. A., & Baldo, J. B. (2014). The behavior of zeta potential of silica suspensions. *New Journal of Glass and Ceramics*, 04(02), 29–37. <https://doi.org/10.4236/njgc.2014.42004>
- Karra, S., Sebii, H., Yaich, H., Bouaziz, M. A., Blecker, C., Danthine, S., ... Besbes, S. (2020). Effect of extraction methods on the physicochemical, structural, functional, and antioxidant properties of the dietary fiber concentrates from male date palm flowers. *Journal of Food Biochemistry*, 44(6), Article e13202.
- Kim, G. S., Park, H. J., Woo, J. H., Kim, M. K., Koh, P. O., Min, W., Ko, Y. G., Kim, C. H., Won, C. K., & Cho, J. H. (2012). *Citrus aurantium* flavonoids inhibit adipogenesis through the akt signaling pathway in 3T3-L1 cells. *Bmc Complementary and Alternative Medicine*, 12, 31.
- Kim, S. H., Hur, H. J., Yang, H. J., Kim, H. J., Kim, M. J., Park, J. H., ... Hwang, J. T. (2013). *Citrus junos* tanaka peel extract exerts antidiabetic effects via AMPK and PPAR-gamma both in vitro and in vivo in mice fed a high-fat diet. *Evidence-Based Complementary and Alternative Medicine*, 2013, Article 921012.
- Kore, V. T., & Chakraborty, I. (2015). Efficacy of various techniques on biochemical characteristics and bitterness of pummelo juice. *Journal of Food Science and Technology-Mysore*, 52(9), 6073–6077.
- Lee, B. B., Kim, Y. M., Pyeon, S. M., Jeong, H. J., Cho, Y. S., & Nam, S. H. (2022). Physicochemical properties and neuroprotective function of korean major yuzu varieties. *Food Science and Technology*, 42, e69222.
- Lee, Y. S., Huh, J. Y., Nam, S. H., Moon, S. K., & Lee, S. B. (2012). Enzymatic bioconversion of citrus hesperidin by *Aspergillus sojae* naringinase: Enhanced solubility of hesperetin-7-O-glucoside with in vitro inhibition of human intestinal maltase, HMG-CoA reductase, and growth of *Helicobacter pylori*. *Food Chemistry*, 135(4), 2253–2259.
- Liu, C. M., Liang, R. H., Dai, T. T., Ye, J. P., Zeng, Z. C., Luo, S. J., & Chen, J. (2016). Effect of dynamic high pressure microfluidization modified insoluble dietary fiber on gelatinization and rheology of rice starch. *Food Hydrocolloids*, 57, 55–61.
- Liu, N., Yang, W., Li, X., Zhao, P., Liu, Y., Guo, L., Huang, L., & Gao, W. (2022). Comparison of characterization and antioxidant activity of different citrus peel pectins. *Food Chemistry*, 386, Article 132683.
- Liu, Y. L., Zhang, H. B., Yi, C. P., Quan, K., & Lin, B. P. (2021). Chemical composition, structure, physicochemical and functional properties of rice bran dietary fiber modified by cellulase treatment. *Food Chemistry*, 342, Article 128352.
- Lv, J. S., Liu, X. Y., Zhang, X. P., & Wang, L. S. (2017). Chemical composition and functional characteristics of dietary fiber-rich powder obtained from core of maize straw. *Food Chemistry*, 227, 383–389.
- Lynch, J. M., & Barbano, D. M. (1999). Kjeldahl nitrogen analysis as a reference method for protein determination in dairy products. *Journal of Aoac International*, 82(6), 1389–1398.
- Ma, M., & Mu, T. (2016). Modification of deoiled cumin dietary fiber with laccase and cellulase under high hydrostatic pressure. *Carbohydrate Polymers*, 136, 87–94.
- Ma, S., Ren, B., Diao, Z., Chen, Y., Qiao, Q., & Liu, X. (2016). Physicochemical properties and intestinal protective effect of ultra-micro ground insoluble dietary fiber from carrot pomace. *Food Function*, 7(9), 3902–3909.
- Ma, W., Liang, Y., Lin, H., Chen, Y., Xie, J., Ai, F., ... Yu, Q. (2023). Fermentation of grapefruit peel by an efficient cellulose-degrading strain, (*Penicillium* YZ-1): Modification, structure and functional properties of soluble dietary fiber. *Food Chemistry*, 420, Article 136123.
- Nam, S. H., Cho, H. S., Jeong, H., Lee, B. B., Cho, Y. S., Rameeza, F., & Eun, J. B. (2021). Physicochemical properties, dietary fibers, and functional characterization of three yuzu cultivars at five harvesting times. *Food Science and Biotechnology*, 30(1), 117–127.
- Peerajit, P., Chiewchan, N., & Devahastin, S. (2012). Effects of pretreatment methods on health-related functional properties of high dietary fibre powder from lime residues. *Food Chemistry*, 132(4), 1891–1898.
- Poudel, B., Nepali, S., Xin, M., Ki, H. H., Kim, Y. H., Kim, D. K., & Lee, Y. M. (2015). Flavonoids from *Triticum aestivum* inhibit adipogenesis in 3T3-L1 cells by upregulating the insig pathway. *Molecular Medicine Reports*, 12(2), 3139–3145.
- Prosky, L., Asp, N. G., Schweizer, T. F., Devries, J. W., & Furda, I. (1988). Determination of insoluble, soluble, and total dietary fiber in foods and food products: Interlaboratory study. *Journal of the Association of Official Analytical Chemists*, 71(5), 1017–1023.
- Sain, M., & Panthapulakkal, S. (2006). Bioprocess preparation of wheat straw fibers and their characterization. *Industrial Crops and Products*, 23(1), 1–8.
- Seong, H. J., Im, A. E., Kim, H., Park, N., Yang, K. Y., Kim, D., & Nam, S. H. (2023). Production of prunin and naringenin by using naringinase from *Aspergillus oryzae* NYO-2 and their neuroprotective properties and debitterization. *Journal of Agricultural and Food Chemistry*, 71(3), 1655–1666.
- Sharma, K., Adhikari, D., Kim, H. J., Oh, S. H., Oak, M. H., & Yi, E. (2019). Fruit extract facilitates anti-adipogenic activity of extract in 3T3-L1 adipocytes by reducing oxidative stress. *Journal of Nanoscience and Nanotechnology*, 19(2), 915–921.
- Song, L. W., Qi, J. R., Liao, J. S., & Yang, X. Q. (2021). Enzymatic and enzyme-physical modification of citrus fiber by xylanase and planetary ball milling treatment. *Food Hydrocolloids*, 121, Article 107015.
- Theuwissen, E., & Mensink, R. P. (2008). Water-soluble dietary fibers and cardiovascular disease. *Physiology Behavior*, 94(2), 285–292.
- Wang, Y., Choi, K. D., Yu, H., Jin, F., & Im, W. T. (2016). Production of ginsenoside F1 using commercial enzyme cellulase KN. *Journal of Ginseng Research*, 40(2), 121–126.
- Wu, C. H., Yang, M. Y., Chan, K. C., Chung, P. J., Ou, T. T., & Wang, C. J. (2010). Improvement in high-fat diet-induced obesity and body fat accumulation by a *Nelumbo nucifera* leaf flavonoid-rich extract in mice. *Journal of Agricultural and Food Chemistry*, 58(11), 7075–7081.
- Yu, G. Y., Bei, J., Zhao, J., Li, Q. H., & Cheng, C. (2018). Modification of carrot (*Daucus carota* Linn. var. *sativa* hoffm.) pomace insoluble dietary fiber with complex enzyme method, ultrafine comminution, and high hydrostatic pressure. *Food Chemistry*, 257, 333–340.
- Zhang, M., Bai, X., & Zhang, Z. S. (2011). Extrusion process improves the functionality of soluble dietary fiber in oat bran. *Journal of Cereal Science*, 54(1), 98–103.
- Zhang, Y., Qi, J. R., Zeng, W. Q., Huang, Y. X., & Yang, X. Q. (2020). Properties of dietary fiber from citrus obtained through alkaline hydrogen peroxide treatment and homogenization treatment. *Food Chemistry*, 311, Article 125873.
- Zheng, Y., & Li, Y. (2018). Physicochemical and functional properties of coconut (*Cocos nucifera* L) cake dietary fibres: Effects of cellulase hydrolysis, acid treatment and particle size distribution. *Food Chemistry*, 257, 135–142.
- Zhu, Y. P., Jia, H. Y., Xi, M. L., Li, J. L., Yang, L., & Li, X. T. (2017). Characterization of a naringinase from *Aspergillus oryzae* 11250 and its application in the debitterization of orange juice. *Process Biochemistry*, 62, 114–121.